

Investigating Fourier Optics and Spatial Filtering

Aritra Mukhopadhyay

National Institute of Science Education and Research

Bhubaneswar, Odisha 751005, India

4th year, Integrated M.Sc. Physics

Roll No.: 2011030

(Dated: March 8, 2024)

In this Fourier Optics Open Lab experiment, our journey unfolded with a foundational understanding of Fourier transforms and the compilation of necessary equipment. Following this, we engaged in the design and 3D printing of custom components, optimizing our experimental setup. Notably, we achieved successful alignments, generating Fourier transform images of diverse objects. The subsequent phase involved comprehensive exploration of filters, leading to the selective isolation of features in letters 'V' and 'H'. Iterative adjustments to laser-cut objects and a strategic modification in the optical path underscored our commitment to refining and advancing our experiment.

I. INTRODUCTION

The investigation of light diffraction encompasses various methodologies predicated upon the wave-like characteristics of light. One may employ the Huygens-Fresnel principle or leverage the comprehensive contributions of Sommerfeld and Kirchhoff to elucidate the physical manifestations of interference and diffraction. The scholarly endeavours of Sommerfeld and Kirchhoff, in particular, have proven highly advantageous in modelling the propagation of light across diverse configurations, either through analytical means or numerical simulations. Moreover, their work has laid the groundwork for Fourier Optics, a discipline centred on the examination of wave phenomena through Fourier Transforms, wherein complex waveforms are conceptualized as compositions of plane waves.

In this experimental inquiry, we have systematically delved into the realm of Fourier Optics within the far-field limit, denoted as the Fraunhofer Diffraction regime. Initially, we derived the correlation between the two-dimensional Fourier transform and Fraunhofer Diffraction, subsequently substantiating the anticipated waveforms through a practical implementation employing a 4f imaging System, as illustrated in Figure 1. A schematic depiction of the experimental arrangement, along with pertinent observations gleaned from the setup, has been provided.

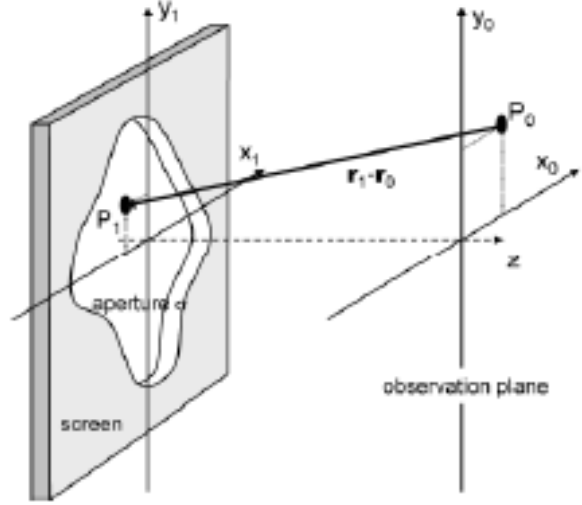


FIG. 2: Transmission through an aperture

The 4f-Imaging System (As in Fig 1), a thoroughly investigated optical image processor, served as the focal point of our exploration. Throughout this experiment, we scrutinized various facets of the system and formulated a numerical model under the paraxial approximation. Our findings indicate that the intricacies of the Fraunhofer regime can be effectively encapsulated through the framework of Fourier Optics. Furthermore, our investigation extended to practical applications of this setup and Fourier Optics more broadly. Notably, we addressed applications such as Spatial Filtering (Optical Image Filtration), Character Recognition, Phase-Contrast Imaging, and Dark-Field Illumination.

In the next section, we expand on the theory of Fourier Optics and briefly explain the aforementioned use cases. Then, in Section - II, we detail the apparatus and procedure for this experiment, and in Section - III, we present our observations. Ultimately, in Section - IV, we discuss our results as well as the experimental setup. We have also presented some extensions to this experiment in the same section. The appendices, containing the code for

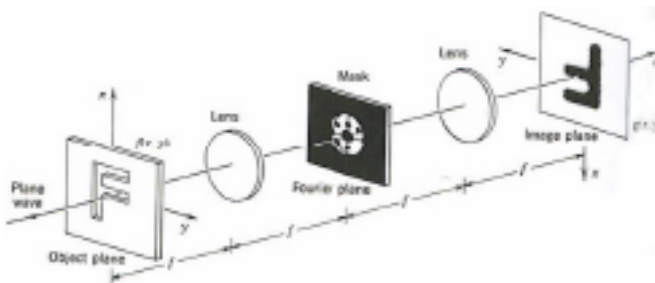


FIG. 1: 4f-Imaging System

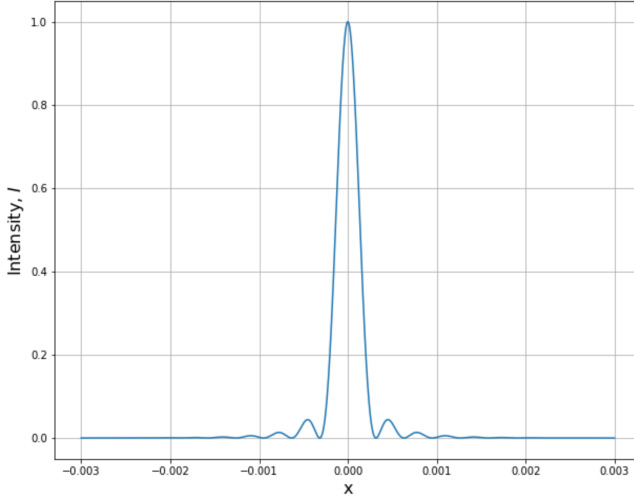


FIG. 3: Intensity profile for a rectangular aperture (along x) (e.g. single slit)

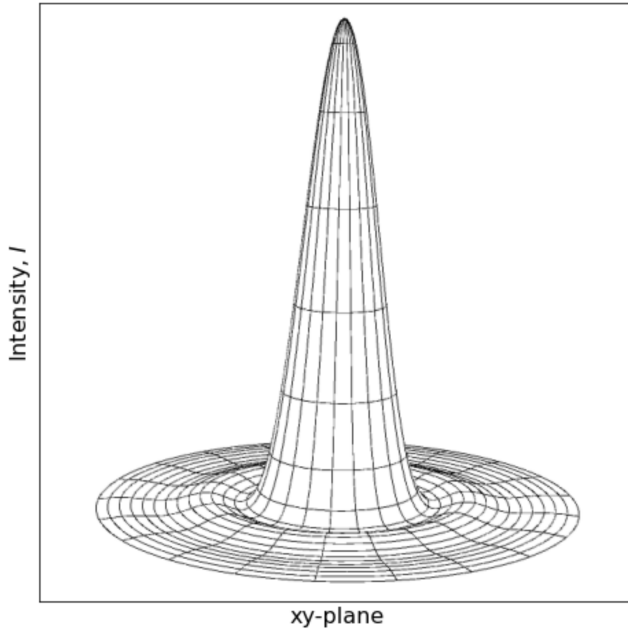


FIG. 4: Intensity profile for a circular aperture (in the xy-plane) (e.g. pinhole)

the numerical model for each case study, can be found near the end of this document.

A. Fraunhofer Diffraction Formula

For a monochromatic wave incident on an aperture, the Rayleigh-Sommerfeld diffraction formula can be given as follows:

$$U(P_0) = \int \int_{\sigma} h(P_0, P_1) U(P_1) ds_1 \quad (1)$$

where,

$$h(P_0, P_1) = -\frac{1}{i\lambda} \cos(n, r_1 - r_0) \frac{e^{-ik|r_1 - r_0|}}{|r_1 - r_0|} \quad (2)$$

$h(P_0, P_1)$ can be thought of as a weight, that is applied to the field, $U(P_1)$ to get the field $U(P_0)$.

Now let us consider a setup as shown in Fig 2. Then, we can write the field at P_0 as:

$$U(P_0) = \int \int_{\sigma} h(x_0, y_0, x_1, y_1) U(x_1, y_1) dx_1 dy_1 \quad (3)$$

with

$$h(x_0, y_0, x_1, y_1) = -\frac{1}{i\lambda} \cos(n, r_1 - r_0) \frac{e^{-ik|r_1 - r_0|}}{|r_1 - r_0|} \quad (4)$$

Also, $|r_1 - r_0| = \sqrt{(x_0 - x_1)^2 + (y_0 - y_1)^2 + z^2}$. If we assume the axial distance (along z) to be much larger than transverse dimensions, then we also have $\cos(n, r_1 - r_0) \approx 1$. We can also expand the square root in a binomial expansion. Retaining terms till order 2, we get:

$$\begin{aligned} |r_1 - r_0| &= \sqrt{(x_0 - x_1)^2 + (y_0 - y_1)^2 + z^2} \\ &\approx z \left[1 + \frac{1}{2} \left(\frac{x_1 - x_0}{z} \right)^2 + \frac{1}{2} \left(\frac{y_1 - y_0}{z} \right)^2 \right] \end{aligned} \quad (5)$$

Substituting back into Eq 4 we get:

$$h(x_0, y_0, x_1, y_1) \approx -\frac{e^{-ikz}}{i\lambda z} e^{-i\frac{k}{2z}[(x_1 - x_0)^2 + (y_1 - y_0)^2]} \quad (6)$$

Finally, we can replace integration over the aperatus(σ) by integration over the entire plane by defining $U(x_1, y_1) = 0$ outside σ . Using this condition and rearranging, we finally obtain:

$$\begin{aligned} U(x_0, y_0) &= -\frac{e^{-ikz}}{i\lambda z} e^{-i\frac{k}{2z}[x_0^2 + y_0^2]} \times \\ &\int \int_{-\infty}^{\infty} U(x_1, y_1) e^{-i\frac{k}{2z}[x_1^2 + y_1^2]} e^{i\frac{2\pi i}{\lambda z}[x_0 x_1 + y_0 y_1]} dx_1 dy_1 \end{aligned} \quad (7)$$

Eq 7 is known as the Fresnel Diffraction integral, and from its form, one can clearly see that the field $U(x_0, y_0)$, in the observation plane, is a 2D Fourier transform of the field in the object plane, $U(x_1, y_1) e^{\frac{2\pi i}{\lambda z}[x_0 x_1 + y_0 y_1]}$, where

the spatial frequencies are defined by: $f_x = -\frac{x_0}{\lambda z}$ and $f_y = -\frac{y_0}{\lambda z}$.

$$z \gg \frac{k}{2}(x_1^2 + y_1^2)_{max} \quad (8)$$

Using this, we can neglect the quadratic phase term, giving us the Fraunhofer Diffraction formula:

$$U(x_0, y_0) = -\frac{e^{-ikz}}{i\lambda z} e^{-i\frac{k}{2z}[x_0^2 + y_0^2]} \int_{-\infty}^{\infty} \int_{-\infty}^{\infty} U(x_1, y_1) e^{i\frac{2\pi}{\lambda z}[x_0 x_1 + y_0 y_1]} dx_1 dy_1 \quad (9)$$

B. Fresnel Number

Now equipped with expressions for diffraction in near and far-field regimes, we introduce the Fresnel Number (F-Number) to determine the applicable diffraction regime:

$$F = \frac{a^2}{L\lambda} \quad (10)$$

where $F \gg 1$ implies near-field diffraction, $F \approx 1$ implies far-field diffraction

In our case, the use of multiple lenses aims to work in the far-field regime by reducing F .

In far-field diffraction, a monochromatic wave passing through an aperture results in a Fourier transform. Spatial Filtering involves designing filters to block specific spatial modes, influencing information in position or phase space. The Convolution Theorem is foundational, expressing the inverse Fourier transform of a convolution as the pointwise product of Fourier transforms:

$$h(x) = \{f * g\}(x) = \mathcal{F}^{-1}\{\mathcal{F}(f) \cdot \mathcal{F}(g)\} \quad (11)$$

Spatial filters compute the ‘overlap’ between the incident wave and the filter, modifying the diffraction pattern. Applications include Low and High-pass filters, Dark-Field Illumination, Phase-Contrast Imaging, and Fourier Descriptors for image encoding.

C. Coherence of Incident Light

In order to obtain well-defined and stationary information in phase space, it is imperative that the incident beam or light source exhibits coherence. Specifically, this coherence should encompass both spatial and temporal aspects. Spatial coherence ensures the existence of stationary spatial modes, while temporal coherence implies a monochromatic wave. Under these conditions, the

wave can undergo Fourier decomposition, as expressed in Equation 9. Conversely, for incoherent waves, where there is no fixed phase relation between two spatial points, Fourier transforms are still applicable. However, the outcome no longer represents a Fourier decomposition into fixed-frequency plane waves. Instead, it becomes a superposition of various monochromatic, coherent contributions, resulting in uniform illumination at the observation screen rather than a discernible diffraction pattern.

D. Fast Fourier Transform

As part of this experiment, we have used the ImageJ software [1] to calculate Fourier and Inverse Fourier transforms of observed images. We have also written Python code to simulate a 4f -Imaging Processor, under paraxial and far-field approximations. We have based our code on a Python library called diffractio [2]. Our Python code can be found in our [GitHub repository](#). Both ImageJ and diffractio make use of Fast Fourier Transform (FFT), which is a divide-and-conquer algorithm, first devised by James W. Cooley and John W. Tukey [3], to make Fourier coefficient computations efficient. More information on FFT, including a bare-bones implementation can be found in [4].

II. METHODOLOGY

A. Apparatus

1. For 4-f imaging system:
 - (a) 2 Optical Benches (one 1m and one 50cm) and holders
 - (b) Ready-made Objects like mesh, pin hole, single and double slits etc.
 - (c) 3D printed custom holders for the above objects and paper objects and filters
 - (d) He-Ne LASER ($15mW$), with $\lambda = 633$ nm
 - (e) Beam Expander, with $f = 50$ mm
 - (f) Collimating Spherical Lens, with $f = 300$ mm
 - (g) 2 Fourier Transform Spherical Lenses, with $f = 300$ mm
 - (h) Observation Screen
2. For creating or modifying objects and filters:
 - (a) Black Chart Paper
 - (b) Laser cutter from RTC to make very fine and complex shapes with precision on the Black chart paper
 - (c) Printed objects and filters from previous batch
3. Mobile Phone camera to record diffraction patterns and reconstructed images.

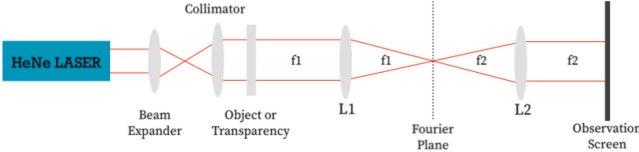


FIG. 5: Schematic of the Experimental Setup

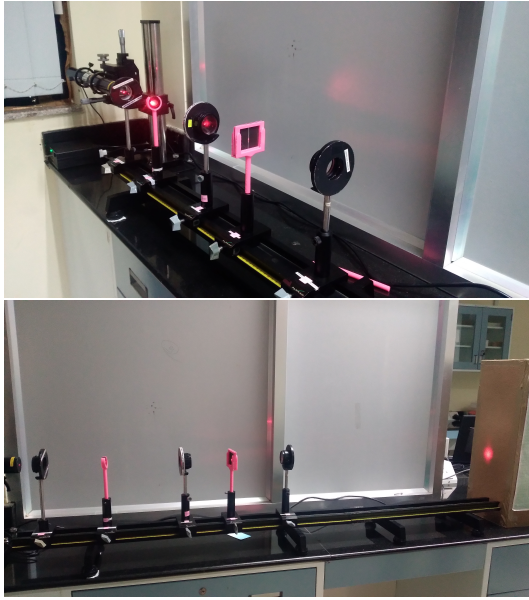


FIG. 6: Photo of the Experimental Setup

B. Experimental Setup

The experimental Setup consists of a 4f-Imaging System, whose schematic has been presented in Fig 5. The actual setup has been displayed in Figure 6. ‘4f’ in the name comes from the fact, that the objective, Fourier transform lenses and the observation screen span a total of 4 focal lengths. In our case, $f_1 = f_2$, but in general, f_1 need not be the same as f_2 .

After expanding and collimating the laser light, it is directed onto a transparency or object. The light then passes through lens L1, producing the Fourier-decomposition or diffraction pattern at the focus of L_1 , known as the Fourier plane. Filters are applied in the Fourier plane to selectively obscure certain spatial modes. Subsequently, lens L2 produces another Fourier transform (or, by asymmetry, the negative of the Inverse Fourier transform), resulting in an inverted microscopic image of the object at the focus of L2. The observation screen (S) can be placed at this focus or, alternatively, a beam expander can be used to generate a magnified and erect image.

If a beam-expanding lens is employed, it results in a Fourier decomposition in the far-field limit. Therefore, the observation screen must be positioned sufficiently close to the beam-expanding lens to observe the magnified

image rather than its diffraction pattern. To enhance visibility, beam expanders are used at both the Fourier plane and the Observation plane, ensuring sharper images in the presented observations.

The 4f-imaging system is beneficial for studying Spatial Filtering in a compact setup. For example, considering diffraction at a 0.5mm wide slit without Fourier Transform lenses, the discussion on the Fresnel Number (Eq. 10) indicates that far-field approximations are valid only for $L > 39.49$ cm. With a lens, the Fourier Transform of the slit function, equivalent to the Fraunhofer diffraction pattern, can be obtained at the focus, reducing the required setup footprint significantly.

We use [OnShape](#) to design and 3D print the holders. Here are links to their OnShape documents:

- Circular holder for the filters: [circle holder](#)
- Holder version 1 for paper filters: [Holder v1](#)
- Holder version 2 for paper filters: [Holder v2](#) Brackets for use with both Holder versions: [brackets](#)

C. Experiments

D. Basic Filters

In the course of our experimentation, we systematically explored various fundamental filters, capturing a multitude of photographs to document our findings. The visual representations encompass essential phenomena such as the Fourier transform of a pinhole 7, the intricate patterns arising from a double slit 8, and the subsequent reconstruction of the double-slit configuration 9. Additionally, we delved into the Fourier transform 10 and reconstruction of a mesh 11, capturing both the overall pattern and a nuanced perspective—allowing only the central vertical set of dots to pass through 14. We also did the fourier transform of a grating 13

The collection of images presented here offers a glimpse into the intriguing world of diffraction patterns and spatial filtering, each photograph telling a unique story of light manipulation and wave interactions.

E. Character Filtering

In pursuit of a novel approach to spatial filtering, we devised a plan to select two distinct characters, each presenting unique features in the Fourier plane. The goal was to construct filters that could selectively mask certain characteristics during the Fourier transform and subsequently remove one character from the reconstructed image.

After exploring various options using ImageJ software, we identified the letters V and H as ideal candidates for our experiment. The rationale behind this choice lay in their dissimilarity in the Fourier plane. Specifically, we

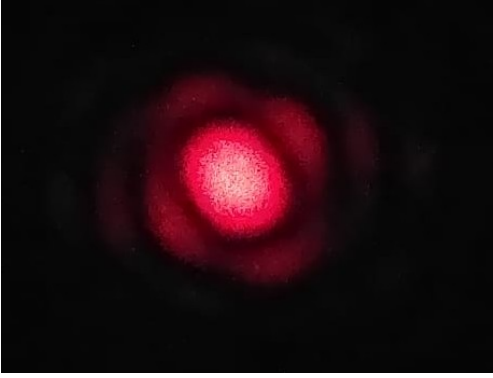


FIG. 7: Fourier Transform of Pin Hole

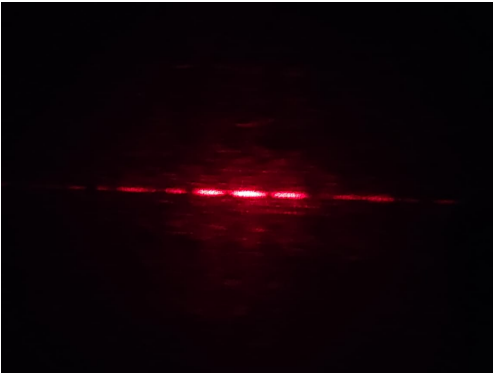


FIG. 8: Fourier Transform of double Slit

anticipated a cross (\times) pattern for the letter V and a plus (+) pattern for the letter H. The inherent dissimilarity in their Fourier transforms made it feasible to create filters that could effectively separate these two characters during the reconstruction process.

To materialize these characters, we opted for precision and efficiency by utilizing a laser cutter. The designs for

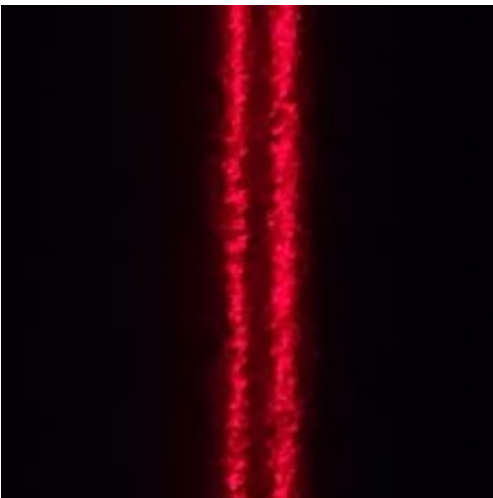


FIG. 9: Reconstruction of Double Slit

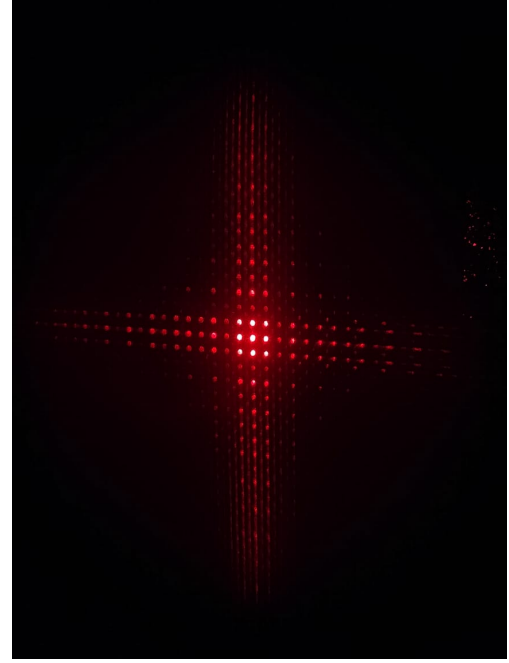


FIG. 10: Fourier Transform of Fine Mesh

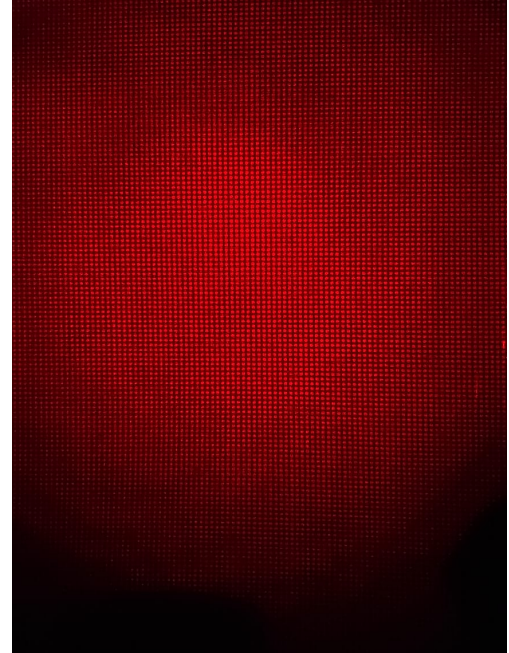


FIG. 11: Reconstruction of Mesh

V and H were crafted in Onshape and exported as .dxf files. The laser cutter then cut these shapes into a thick black chart paper. Notably, we produced two variations of each character: one at the original size and two additional versions scaled 2X and 3X larger.

Figure 15 visually encapsulates the Fourier transform of the VH object, portraying the distinctive patterns we anticipated. However, our primary objective was to selec-

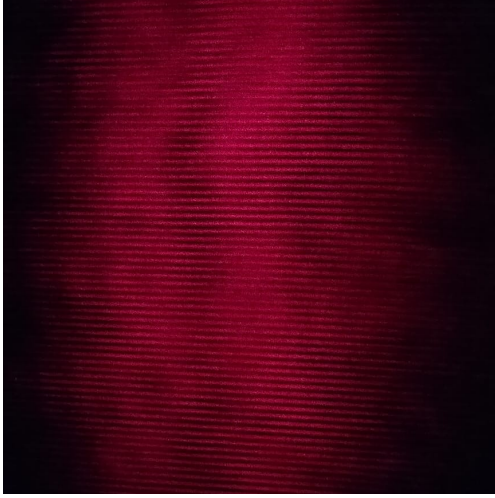


FIG. 12: Mesh Reconstruction, but we only let the central vertical set of dots pass through



FIG. 13: Fourier Transform of a vertical grating

tively remove either the letter V or H during the reconstruction phase. This intricate process involved the design and implementation of specialized filters to achieve our desired outcomes, showcased in Figures 16 and 17.

In our endeavor to preserve specific features and eliminate unwanted elements, we recognized the significance of the central dot in the Fourier plane. While it contained

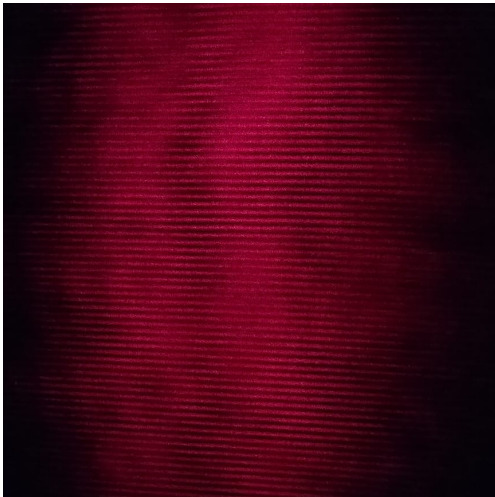


FIG. 14: Mesh Reconstruction, but we only let the central vertical set of dots pass through

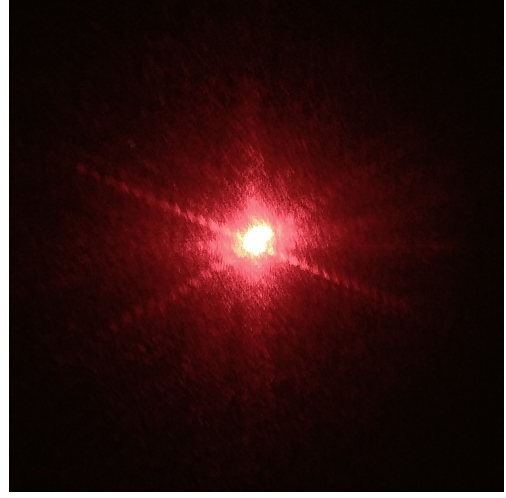


FIG. 15: Fourier Transform of VH Object

valuable information, we sought to remove it to enhance the selectivity of our filters. For the filter designed to retain the letter V, we crafted a pattern featuring four long holes arranged in a cross configuration, with the central region remaining unaltered. This design allowed us to selectively preserve the Fourier transform characteristics associated with the letter V.

Conversely, for the filter tailored to retain the letter H and eliminate V, we engineered a pattern with four long holes arranged in a plus fashion, with the central area remaining intact. By strategically positioning the holes, we effectively filtered out the Fourier transform features related to the letter V, resulting in the reconstructed image shown in Figure 17.

Figure 18 visually represents the designed filters: one for selectively keeping V and the other for retaining H while removing V. These intricate patterns were meticulously crafted to ensure the preservation of specific spatial features in the Fourier plane, contributing to the successful realization of our experimental goals.

We also tried to remove a major part from the center of the Fourier Transform, the reconstructed image looks like Figure 19

III. DISCUSSIONS AND CONCLUSION

- **Spatial Features in Fourier Transform:** Our observations underscore the distinctive behavior of spatial features in the Fourier transform. A straight line in the image results in a diffraction pattern rotated by 90 degrees. When multiple straight lines are present, they superimpose on each other. This insight is crucial in understanding how spatial characteristics manifest in the frequency domain.

- **Loss of Relative Spatial Features:** The Fourier transform exhibits a loss of relative spatial features. For instance, the Fourier transform of the letters T



FIG. 16: Reconstructed Image with V Removed



FIG. 17: Reconstructed Image with H Removed

and L is identical, erasing information about the vertical positioning of the horizontal line. However, during image reconstruction, these differences become discernible. This emphasizes the importance of considering both transform and inverse transform phases for a comprehensive understanding.

- **Selective Removal of Horizontal Features:** The ability to remove horizontal features universally by introducing a single vertical wire in the Fourier transform plane highlights the power of spatial filtering. This manipulation is grounded in the fundamental principles of Fourier optics and provides a practical method for altering image characteristics.
- **Central Brightness and Low-Frequency Fea-**

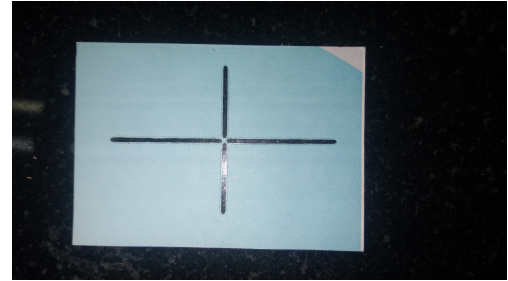


FIG. 18: Designed Filters for Selective Removal

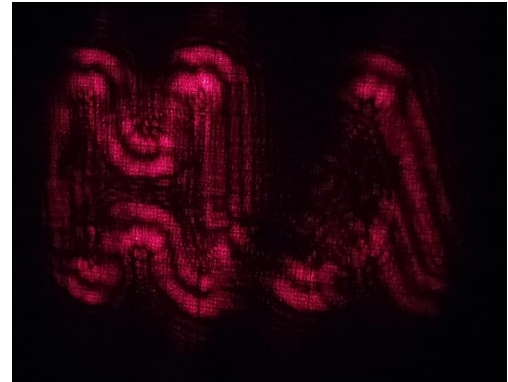


FIG. 19: Reconstructed VH, with high pass filter

tures: The central part of the Fourier transform, characterized by its brightness, plays a pivotal role in determining the overall brightness of the image. Removing the central region from the Fourier transform, especially for an object with a square hole, results in a dim square border with both the center and the outer regions appearing dark. This aligns with the expected behavior of low-frequency features in the frequency domain.

- **Information Content in Bright Dots:** Brighter dots in the Fourier transform carry more information than dimmer ones. This observation resonates with the concept that higher intensities in the frequency domain correspond to more prominent features in the spatial domain, providing valuable insights into the relationship between brightness and information content.
- **Challenges in Filtering Circular Features:** The circular nature of the letter "O" poses challenges for filtering, as it has features in all directions. Consequently, attempts to filter out "O" will inherently pass a significant portion of its character. This highlights the intricacies involved in filtering circular patterns and the need for tailored approaches in such scenarios.

IV. ERRORS AND ISSUES IN THE SETUP

A. Setup: Issues & Improvements

1. Sustained Coherence of Light

a. *Issue:* The experiment requires sustained coherence of the light source over the setup dimensions. However, back-reflection and optical cavity effects were observed, particularly noticeable with spherical lenses, potentially compromising coherence.

b. *Improvement:* To enhance coherence, alternatives such as using Aspheric lenses or incorporating an Aperture Stop were suggested. A recommended coherence test involving only essential components (LASER, beam expander, collimator, and observation screen) helps assess the coherence of the light beam.

2. High Beam Intensity

a. *Issue:* High beam intensity posed challenges during data collection, necessitating adjustments to camera settings and causing inconsistencies across images.

b. *Improvement:* Lowering the LASER intensity was proposed to improve experiment performance and facilitate the standardization of camera settings, ensuring more consistent data collection.

3. Narrow Beam

a. *Issue:* The available beam expanders did not produce a sufficiently wide beam, restricting effective experimentation, particularly with larger images.

b. *Improvement:* To address this limitation, suggested solutions include exploring alternative beam expanders or collimators. Additionally, considering a higher wavelength source was proposed to widen the beam. While this may reduce coherence length, the use of high-magnification lenses could help mitigate this effect, ultimately expanding the setup's capabilities.

These proposed improvements aim to rectify issues related to coherence, beam intensity, and beam width, contributing to the optimization of the 4f-imaging system for more reliable and versatile experiments.

V. FUTURE EXTENSIONS

A. Machine Learning

This experiment lays the groundwork for various future extensions. One promising avenue is the integration of Fourier decomposition into Machine Learning methodologies. The unique Fourier descriptors for each character or alphabet, whether in position or phase space, present an opportunity for more efficient data encoding. Leveraging this property in Machine Learning applications, particularly in character recognition, could offer speed advantages over traditional algorithms, especially considering the efficiency of Fast Fourier Transform. Beyond character recognition, these Fourier descriptors might find applications in broader image classification problems [5].

B. Transfer Function Formalism

While the concepts of Fourier Optics have been explored through the works of Fresnel and Sommerfeld, a future extension involves adopting a signal processing perspective, particularly through the lens of Transfer Function Formalism. This formalism provides a concise framework to study Fourier Optics and can enhance the understanding of operations such as convolution at an aperture. Additionally, it allows for a more intuitive comprehension of complex phase space information. This conceptual groundwork can be further extended to investigate filters like the VanderLugt Filter [6], matched filters [7], and phase-only filters [8].

C. Information Theoretic Approach

Another avenue for extension involves applying principles from Information Theory to quantify the transfer and loss of information in optical image processors [9, 10]. This approach aims to maximize information content, facilitating better reconstructions of distorted or modified source images. The exploration of Information Theory principles in the context of optical image processing could lead to valuable insights and optimizations.

-
- [1] C. A. Schneider, W. S. Rasband, and K. W. Eliceiri, Nih image to imagej: 25 years of image analysis, *Nature Methods* **9**, 671 (2012).
 - [2] L. M. S. Brea, *diffractio: Python Diffraction-Interference module*.
 - [3] J. W. Cooley and J. W. Tukey, An algorithm for the machine calculation of complex fourier series, *Mathematics of Computation* **19**, 297 (1965).
 - [4] W. H. Press, S. A. Teukolsky, W. T. Vetterling, and B. P. Flannery, *Numerical Recipes 3rd Edition: The Art of Scientific Computing*, 3rd ed. (Cambridge University Press, 2007).
 - [5] Fourier descriptor, auto-generated, ScienceDirect.
 - [6] A. V. Lugt, Signal detection by complex spatial filtering, *IEEE Transactions on Information Theory* **10**, 139 (1964).

- [7] G. Turin, An introduction to matched filters, IRE Transactions on Information Theory **6**, 311 (1960).
- [8] J. L. Horner and P. D. Gianino, Phase-only matched filtering, Appl. Opt. **23**, 812 (1984).
- [9] E. H. Linfoot, Information theory and optical images, J. Opt. Soc. Am. **45**, 808 (1955).
- [10] J. A. O'Sullivan, R. E. Blahut, and D. L. Snyder, Information-theoretic image formation, IEEE Transactions on Information Theory **44**, 2094 (1998).